# Charge-imbalance relaxation in the presence of a pair-breaking interaction in superconducting AlEr films

Thomas R. Lemberger and John Clarke
*Department of Physics, University of California, Berkeley, California 94720*
*and Materials and Molecular Research Division, Lawrence Berkeley Laboratory, Berkeley, California 94720*
(Received 28 July 1980)

The charge-imbalance relaxation rate, $1/F^*\tau_{Q^*}$, has been measured in dirty superconducting AlEr films in which Er is a pair-breaking magnetic impurity that induces charge relaxation through elastic exchange scattering. Measurements were made in the range $0.1 \lesssim \Delta(T)/k_B T_c \lesssim 1.4$ for Er concentrations varying from 21 to 1660 at. ppm that produced estimated exchange scattering rates, $\tau_S^{-1}$, from about $10^9$ sec$^{-1}$ to $5\times10^{10}$ sec$^{-1}$. Measured values of $1/F^*\tau_{Q^*}$ were in good agreement with the Schmid-Schön expression, $1/F^*\tau_{Q^*} = (\pi\Delta/4k_B T_c\tau_E) \times (1+2\tau_E/\tau_S)^{1/2}$, for $\Delta/k_B T_c \lesssim 0.8$, where $\tau_E^{-1}$ is the electron-phonon scattering rate estimated from the measured transition temperature. For larger values of $\Delta/k_B T_c$, the relaxation rate increased less rapidly with $\Delta$. The appropriate Boltzmann equation was solved on a computer to obtain values for $1/F^*\tau_{Q^*}$ in the range $0.5 \leq T/T_c \leq 0.999\,999$. The computed values of $1/F^*\tau_{Q^*}$ agreed with several analytic expressions valid for $\Delta/k_B T_c \ll 1$, but not with the experimental data: The computed curves increased more rapidly than linearly with $\Delta/k_B T_c$ near $T_c$, and the shape of the $1/F^*\tau_{Q^*}$ vs $\Delta/k_B T_c$ curves was qualitatively different. This discrepancy suggests that either the generally accepted expression for exchange charge relaxation is incorrect, or that the Boltzmann equation is inappropriate for these calculations.

## I. INTRODUCTION

A charge imbalance, $Q^*$, exists in a superconductor when a suitable external perturbation causes the density of electronlike excitations to differ from the density of holelike excitations. Examples of such perturbations are: tunnel injection of electrons,[1] electric[2,3] or thermal[4] current flow across a normal-superconductor interface, and supercurrent flow in the presence of a temperature gradient.[5] A charge imbalance is also generated near a phase-slip center.[6] The size of the charge imbalance generated by a perturbation is determined by the size of the perturbation and the rate at which the charge imbalance relaxes through quasiparticle collisions, $\tau_{Q^*}^{-1}$. In the first theoretical analysis of charge-imbalance relaxation, Tinkham[7] studied two mechanisms, namely, inelastic scattering of quasiparticles by phonons and elastic scattering of quasiparticles by nonmagnetic impurities in the presence of an anisotropic energy gap. Tinkham's theory was later extended by Schmid and Schön[8] (SS), Pethick and Smith[9] (PS), and others.[10,11] One important result of the theory is the prediction that for $\Delta/k_B T_c \ll 1$, where $\Delta(T)$ is the order parameter and $T_c$ is the transition temperature, the phonon-mediated relaxation rate is $\tau_{Q^*}^{-1} = \pi\Delta/4k_B T_c\tau_E$. Here, $\tau_E^{-1}$ is the inelastic scattering rate[12] of a quasiparticle at the Fermi energy at $T = T_c$.

Measurements of the phonon-mediated relaxation rate in dirty Sn films[1,13,14] have demonstrated that $\tau_{Q^*}^{-1} \propto \Delta$ in the limit $T \to T_c$, and have yielded reasonable values for $\tau_E^{-1}$, thus lending support to the above theories. Chi and Clarke[15] (CC) investigated both the inelastic and elastic scattering mechanisms in Al by varying the resistivity, and hence the transition temperature of the Al films. They found $\tau_E = 12$ nsec in their cleanest films ($\tau_E = \tau_0/8.4$, where $\tau_0$ is the characteristic inelastic time used by CC), a value that is in good agreement with some other measurements,[16,17] but smaller by as much as a factor of 4 compared with yet other measurements[18–20] and with theoretical estimates.[21,22] Furthermore $\tau_E$ appeared not to depend on either $T_c$ or film resistivity in a reasonable way. CC suggested that the dependence of $\tau_E$ on $T_c$ could be better explained if a small fraction of the elastic scattering were from magnetic impurities, assuming that the analytic SS result for $\tau_{Q^*}^{-1}$ in the presence of magnetic impurities (discussed below), were valid. They also found good agreement between the measured charge relaxation rate for samples in which elastic scattering from nonmagnetic impurities contributed significantly to $\tau_{Q^*}^{-1}$ and a computer model based on the Boltzmann equation. However, they required rather large values of their fitting parameter, the mean-square gap anisotropy for pure Al, than is expected.

The SS theory,[8] valid for $T$ near $T_c$, was the first to include the effect of a pair-breaking mechanism on $\tau_{Q^*}^{-1}$. Subsequently, Kadin *et al.*[23] measured the resistance generated by phase-slip centers in thin Sn films, with pair-breaking generated by a magnetic field parallel to the film. Hsiang[24] measured the resistance of *NS* interfaces between PbBi and Cd, with pair-breaking induced by a magnetic field parallel to the interface. Both experiments demonstrated convincingly that pair-breaking contributed to charge relaxation, and gave support to the SS theory. However, due to uncertainties in the interpretation of the data, neither experiment provided a detailed and quantitative test of the theory. The main objectives of the present investigation are first, to measure $\tau_{Q^*}^{-1}$ as a function of $\Delta(T)/k_B T_c$ in films of AlEr in which the Er provides a pair-breaking mechanism, and second, to extend the theory numerically to temperatures below the restricted range near $T_c$ in which the SS result is valid. In the numerical calculation, we solve the Boltzmann equation used by CC with an additional term for exchange scattering, and use the computed quasiparticle distribution function to calculate $\tau_{Q^*}^{-1}$.

The outline of the paper is as follows. Section II contains the relevant theoretical background necessary for interpreting the experiment and, in particular, for understanding the effects of magnetic impurities on $\tau_{Q^*}^{-1}$. In Secs. III and IV we present the experimental procedures and results, and compare the results with the analytic SS expression. In Sec. V we describe the numerical calculation and compare the results with the SS theory and with our data. Section VI is our concluding summary.

## II. THEORETICAL BACKGROUND

In this section, we review the relevant details of charge-imbalance generation and detection with tunnel junctions, and of charge-imbalance relaxation. The quantity $Q^*$ is defined by the quasiparticle distribution function $f_{\vec{k}\sigma}$, referring to the state $\vec{k}$ with spin $\sigma$, through the relation

$$Q^* = \frac{1}{\Omega} \sum_{\vec{k}\sigma} q_{\vec{k}} f_{\vec{k}\sigma} \quad . \tag{2.1}$$

Here, $q_{\vec{k}} = \epsilon_{\vec{k}}/E_{\vec{k}}$ is the effective quasiparticle charge, $\epsilon_{\vec{k}} = k^2/2m - \mu_s$, $E_{\vec{k}} = +(\epsilon_{\vec{k}}^2 + \Delta^2)^{1/2}$, $\mu_s$ is the chemical potential of the condensate, $\Delta$ is the order parameter, and $\Omega$ is the volume under consideration. The value of $\mu_s$ is determined by requiring that the total electron density be the same in the presence of a charge imbalance as it is in thermal equilibrium. Waldram[10] showed that this condition requires

$$Q^* = -2N(0)\delta\mu_s \quad , \tag{2.2}$$

where $\delta\mu_s$ is the difference between the actual value of $\mu_s$ and its value in thermal equilibrium, and $N(0)$ is the normal-state density of electron states for a single spin. Thus, measurements of $Q^*$ are measurements of $\delta\mu_s$.

In our experiment, charge imbalance is generated by injecting quasiparticles into the superconductor across a tunnel barrier. The rate of injection of quasiparticle charge is

$$\dot{Q}_i^* = \frac{2}{\Omega} \sum_{\vec{k}} q_{\vec{k}} \dot{f}_{\vec{k}}|_i \tag{2.3}$$

where $\dot{f}_{\vec{k}}|_i$ is the rate at which quasiparticles are injected into the state $\vec{k}$, and the sum over spin has been performed. Equation (2.3) can be written in the form[9]

$$\dot{Q}_i^* = F^* I_i / e\,\Omega \quad , \tag{2.4}$$

where $F^*(\Delta, \Delta', V_i)$ is a calculable function that has the limiting form

$$F^* \approx 1 - \pi\Delta/|2eV_i| \quad (|eV_i| >> k_B T, \Delta, \Delta') \quad . \tag{2.5}$$

Here, $I_i$ and $V_i$ are the current through and voltage across the injector junction, $\Delta'$ is the energy gap in the injector film and $e = -|e|$ is the electronic charge. In the experiments and calculations reported in this paper, $F^*$ varies between 0.95 and 1. Since this is a steady-state experiment in which $Q^*$ is uniformly distributed over the volume $\Omega$, we can define a relaxation rate $1/\tau_{Q^*} \equiv \dot{Q}_i^*/Q^*$. Because one measures $I_i/e\,\Omega$ rather than $\dot{Q}_i^*$, it is convenient to present the measurements in the form

$$1/F^*\tau_{Q^*} = I_i/e\,\Omega Q^* \quad . \tag{2.6}$$

One detects $Q^*$ by means of a tunnel junction between the superconductor and a normal metal. When a charge imbalance exists in the volume of the superconductor adjacent to the tunnel barrier, a voltage $V_d$ must be applied across the junction to keep the current through the junction zero. This voltage is related to $Q^*$ by[7]

$$Q^* = 2N(0)eV_d g_{NS} \quad , \tag{2.7}$$

where $g_{NS}(0,T)$ is the zero-voltage conductance $G_{NS}(0,T)$ of the detector junction normalized to its value at the transition temperature, $T_c$. Combining Eqs. (2.6) and (2.7) we find

$$1/F^*\tau_{Q^*} = I_i/2N(0)e^2\Omega g_{NS} V_d \quad . \tag{2.8}$$

We now turn to a discussion of scattering processes that contribute to charge-imbalance relaxation, beginning with those that conserve quasiparticle spin. Phonon scattering involves two types of processes, scattering of a quasiparticle from one energy level to another, and recombination of two quasiparticles. These processes are governed by the coherence fac-

tors $(uu'-vv')^2$ and $(vu'+uv')^2$, respectively, where the primed and unprimed quantities refer to the two states involved in the scattering, $u_{\vec{k}}^2=\frac{1}{2}(1+\epsilon_{\vec{k}}/E_{\vec{k}})$, and $v_{\vec{k}}^2=\frac{1}{2}(1-\epsilon_{\vec{k}}/E_{\vec{k}})$. The coherence factors allow $Q^*$-relaxation processes, with a change in $|Q^*|$ of $|q_{\vec{k}'}-q_{\vec{k}}|$ and $|-q_{\vec{k}'}-q_{\vec{k}}|$ for scattering and recombination, respectively. Charge relaxation may also occur through elastic scattering from one branch to the other, a process that is governed by the coherence factor $(uu'-vv')^2$. It is easy to show that this factor vanishes if the energy gap is isotropic, but that it is nonzero (although still $<<1$) if the gap is anisotropic. In the present experiment, the gap anisotropy is so small that this relaxation mechanism is negligible.

The effect of a pair-breaking interaction on $Q^*$ relaxation is dramatic. A pair-breaking interaction destroys the degeneracy between time-reversed electron states, and thereby gives the Cooper pairs a finite lifetime, the inverse of which is called the pair-breaking rate. In the present work, the pair-breaking mechanism is the exchange interaction between the conduction electrons and magnetic impurities. Abrikosov and Gor'kov[25] showed that the pair-breaking rate is the elastic exchange scattering rate, $\tau_S^{-1}$, for electrons in the normal metal. (This rate is often called the "spin-flip" scattering rate.) Thus, the pair-breaking rate is proportional to the concentration of magnetic impurities. They also demonstrated that a small amount of pair-breaking has several important effects. It smears out the peak in the BCS[26] density of states over an energy range $\hbar\tau_S^{-1}$, so that the energy gap and the order parameter are no longer equal. It also depresses the transition temperature by $\hbar\pi/4k_B\tau_S$, and alters the temperature dependence of the order parameter from the usual BCS form. In the presence of magnetic impurities, charge relaxation can occur because the coherence factor for elastic exchange scattering from one branch to the other in an isotropic, uniform superconductor is not zero, but of the form

$$(uu'+vv')^2=4u^2v^2=\Delta^2/E^2 \quad . \tag{2.9}$$

Since this factor approaches unity as $E\rightarrow\Delta$, we expect the exchange scattering to have an appreciable effect on $\tau_{Q^*}^{-1}$ when $\tau_S^{-1}\gtrsim\tau_E^{-1}$. It is important to realize that, because $\tau_E^{-1}$ is small in Al, a quite small concentration of magnetic impurities ($\hbar\tau_S^{-1}<<k_BT_c$), can produce an exchange scattering rate $\tau_S^{-1}$ that is very much larger than $\tau_E^{-1}$. Hence we are able to add a magnetic impurity, Er, to the Al in amounts which increase $1/F^*\tau_{Q^*}$ by as much as a factor of 10, but change the equilibrium properties of the Al by only a few percent.

SS considered the effect of pair-breaking on $\tau_{Q^*}^{-1}$ and obtained an analytic result for $1/F^*\tau_{Q^*}$ valid when $\Delta/k_BT<<(\tau_E\Gamma)^{-1/2}$, where $\Gamma=\tau_E^{-1}+2\tau_S^{-1}$, that is when $\tau_{Q^*}^{-1}<<\tau_E^{-1}$:

$$\frac{1}{F^*\tau_{Q^*}}=\frac{\pi\Delta}{4k_BT_c\tau_E}\left[1+\frac{2\tau_E}{\tau_S}\right]^{1/2} \quad (\tau_E<<\tau_{Q^*}) \quad . \tag{2.10}$$

In Eq. (2.10), a factor $(1+\hbar^2\Gamma/\Delta^2\tau_E)^{1/2}$ has been omitted since it is very close to unity for all values of $\tau_E$, $\tau_S$, and $\Delta$ used in this experiment. This factor accounts for the effect of the density of states smearing on $\tau_{Q^*}^{-1}$. Note that this smearing is certainly large when $\hbar\tau_S^{-1}\gtrsim\Delta$, but that in the SS picture in the limit $\tau_S^{-1}>>\tau_E^{-1}$ it apparently has little effect on $\tau_{Q^*}^{-1}$ until $\hbar^2\Gamma/\Delta^2\tau_E\gtrsim 1$, or, equivalently, $\hbar/\tau_S\gtrsim\Delta(T)\times(\tau_E/2\tau_S)^{1/2}$. This is a much weaker condition than $\hbar/\tau_S\gtrsim\Delta$.

It will be helpful to our later analysis to interpret Eq. (2.10) physically. First, consider the limit $\tau_S^{-1}<<\tau_E^{-1}$ in which the exchange scattering is a weak perturbation on the inelastic scattering, and to a first approximation does not affect the quasiparticle distribution created by the inelastic processes. Equation (2.10) can be expanded to give

$$\frac{1}{F^*\tau_{Q^*}}=\frac{\pi\Delta}{4k_BT_c}\left[\frac{1}{\tau_E}+\frac{1}{\tau_S}\right] \tag{2.11}$$

$$(\tau_S^{-1}<<\tau_E^{-1},\ \tau_{Q^*}^{-1}<<\tau_E^{-1}) \quad .$$

The phonon-mediated term, $\pi\Delta/4k_BT_c\tau_E$, can be understood by a consideration of the coherence factors that govern charge relaxation by both inelastic scattering and recombination events. One finds that these factors are significantly different from zero only when one of the states is in the range $\Delta\lesssim E\lesssim 2\Delta$. If we further assume the quasiparticles to be uniformly distributed in the energy range $\Delta$ to $k_BT_c$, where $k_BT_c>>\Delta$, then only a fraction $\sim\Delta/k_BT_c$ of the inelastic events contribute to charge relaxation, producing a charge-relaxation rate $\sim\Delta/k_BT_c\tau_E$. The exchange term, $\pi\Delta/4k_BT_c\tau_S$, arises because the coherence factor is substantial only in the energy range from $\Delta$ to roughly $2\Delta$, so that only a fraction $\Delta/k_BT_c$ of the excess quasiparticles can relax. We note here that Pethick and Smith[27] have used a slightly more accurate expression[28] for the exchange scattering operator [see Eq. (5.3)] to obtain

$$\frac{1}{F^*\tau_{Q^*}}=\frac{\Delta}{k_BT_c}\left[\frac{\pi}{4\tau_E}+\frac{1}{\tau_S}\right] \tag{2.12}$$

$$(\tau_S^{-1}<<\tau_E^{-1},\ \tau_{Q^*}^{-1}<<\tau_E^{-1}) \quad .$$

In the limit $\tau_S^{-1}>>\tau_E^{-1}$, Eq. (2.10) reduces to

$$\frac{1}{F^*\tau_{Q^*}}=\frac{\pi\Delta}{4k_BT_c}\left[\frac{2}{\tau_E\tau_S}\right]^{1/2} \tag{2.13}$$

$$(\tau_S^{-1}>>\tau_E^{-1},\ \tau_{Q^*}^{-1}<<\tau_E^{-1}) \quad .$$

In this limit, the exchange scattering modifies the quasiparticle distribution substantially because the lower-energy excess quasiparticles undergo exchange scattering to the other branch more rapidly than higher-energy quasiparticles can cool to replace them. As a result, the energy below which exchange charge relaxation is important is increased from $\sim 2\Delta$ to an energy $E^*$. We estimate this energy by equating the cooling rate, $\sim \tau_E^{-1}$, with the exchange branch crossing rate, $\sim \Delta^2/E^{*2}\tau_S$, to find $E^* \sim \Delta(\tau_E/\tau_S)^{1/2} >> \Delta$. Thus, at temperatures near $T_c$, of the quasiparticles scattered downwards by the cooling process, a fraction $\sim E^*/k_B T_c$ contributes significantly to charge relaxation, so that the rate is $\sim E^*/k_B T_c \tau_E$ $\sim (\Delta/k_B T_c)(\tau_E \tau_S)^{-1/2}$, in essential agreement with Eq. (2.13). We emphasize that $\tau_E^{-1}$ enters the result not because it contributes to the charge relaxation *per se,* but because it determines the rate at which quasiparticles scatter downwards into the region from which they exchange scatter to the other branch. We also note that this picture is valid only if the "fraction" $E^*/k_B T$ is much less than unity, that is, if $(\Delta/k_B T)(\tau_E/\tau_S)^{1/2} << 1$ or $(\tau_E/\tau_{Q^*}) << 1$. This constraint is in accord with SS constraint in Eq. (2.13).

## III. EXPERIMENTAL PROCEDURES

The sample geometry, illustrated in Fig. 1, is very similar to that used by CC. The Al-AlOx-AlEr junction was the injector, and the AlEr-AlOx-Cu junction was the detector. The metal films were 3 mm wide. To eliminate possible edge effects, SiO about 130 nm thick was used to define the injector and detector junction areas to be $1.5 \times 1.5$ and $0.75 \times 0.75$ mm$^2$, respectively, with the detector junction centered over the injector junction. The Al films were from 200 to 400 nm thick, the AlEr films were typically 200 nm thick, while the Cu films were made about 1 $\mu$m thick, to reduce their electrical resistance. The Pb films were also used to measure the resistivity of the AlEr film. The film thicknesses were measured during evaporation with a quartz crystal oscillator, although the quoted values of AlEr were taken as those measured subsequently with an optical interferometer. The Al films were evaporated in the presence of oxygen to increase their transition temperature above those of the AlEr films. The higher transition temperature enabled us to determine the AlEr order parameter from the $I_i$-$V_i$ characteristic of the injector junction for temperatures up to the AlEr transition, and also ensured that the injection current was spatially uniform across the area of the junction. The AlEr films were made by evaporating pellets from a resistively heated tungsten boat. The pellets were cut from a ribbon of AlEr made by rolling a piece of 99.999 at.% pure Al wire into a 0.5-mm

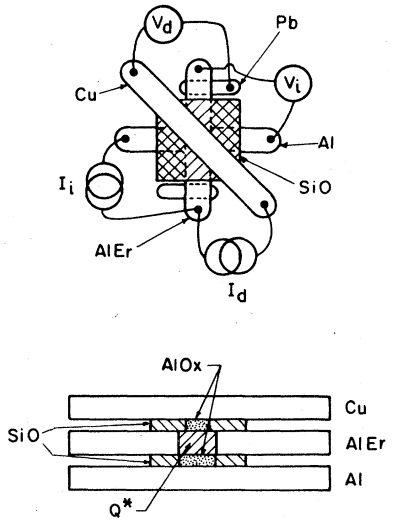


FIG. 1. Sample configuration: plan (top), side (bottom).

thick foil, and evaporating Er onto one side. We estimated the Er concentrations to about ±10% from the relative thicknesses of the Al and Er, assuming bulk values for the densities. The pellets were dropped from a conveyor belt inside the evaporator into a hot tungsten boat. Each pellet evaporated in a few seconds to produce 3 to 5 nm of AlEr film. This procedure produced relatively dirty films with electron mean free paths between 13 and 56 nm, and transition temperatures higher than for bulk Al (see Table I) because the increase in $T_c$ due to dissolved oxygen was greater than the decrease due to magnetic impurities. We estimate that the depression in $T_c$ due to the magnetic impurities in the film with the highest concentrations (0.166 at.%) was about 0.1 K.

We attached wires to each sample to enable us to make four-terminal measurements of $I_i$ vs $V_i$, $dV_i/dI_i$ vs $V_i$, $I_d$ vs $V_d$, and $V_d$ vs $I_i$. The voltage across either junction was defined as positive when the current through that junction flowed into the AlEr film. A dc superconducting quantum interference device (SQUID) voltmeter in a current-nulling feedback mode was used to determine $V_d$. The assembled sample and SQUID were enclosed in a superconducting can to screen out external magnetic field fluctuations, and immersed directly in liquid $^4$He. The temperature of the bath could be lowered to $\sim$1 K by means of a booster pump, and was measured with an Allen-Bradley carbon resistor. The same resistor was used in a feedback circuit[29] with a heater to regulate the bath to about ±100 $\mu$K.

Table I lists the relevant properties of the AlEr films and the resistance of the injector junction, $R_i$. The quantity $R_{300}/R_{4.2}$ is the residual resistivity ratio between 300 and 4.2 K. The electron mean free path, $l$, was determined from the resistivity using[30]

TABLE I. Measured and calculated values for AlEr films.

| Sample No. | Er Concentration $n_{Er}$ (at. ppm) | AlEr film thickness (nm) | $T_c$ (K) | $\frac{R_{300}}{R_{4.2}}$ | $\rho_{4.2}$ (n$\Omega$ m) | $l$ (nm) | $R_i$ ($\Omega$) | $\tau_E$ (nsec) | Estimated $\tau_S$ (psec) | Fitted $\tau_S$ (psec) |
|---|---|---|---|---|---|---|---|---|---|---|
| 1 | 21 | 183 | 1.338 | 2.3 | 25 | 38 | 2.5 | 8.6 | 2500 | 1100 |
| 2 | 21 | 180 | 1.340 | 2.2 | 27 | 36 | 0.9 | 8.6 | 2500 | 1180 |
| 3 | 81 | 200 | 1.276 | 2.7 | 18 | 55 | 4.0 | 9.9 | 650 | 680 |
| 4 | 81 | 210 | 1.277 | 2.7 | 17 | 56 | 4.1 | 9.9 | 650 | 540 |
| 5 | 81 | 184 | 1.350 | 2.1 | 30 | 32 | 2.7 | 8.3 | 650 | 800 |
| 6 | 81 | 175 | 1.350 | 2.1 | 30 | 32 | 2.5 | 8.3 | 650 | 860 |
| 7 | 220 | 205 | 1.410 | 1.8 | 43 | 22 | 1.2 | 7.4 | 240 | 210 |
| 8 | 520 | 204 | 1.507 | 1.4 | 74 | 13 | 1.6 | 6.0 | 93 | 130 |
| 9 | 520 | 199 | 1.507 | 1.4 | 73 | 13 | 1.6 | 6.0 | 93 | 130 |
| 10 | 1660 | 105 | 1.382 | 1.6 | 53 | 18 | 0.9 | 7.8 | 32 | 19 |

$\rho_{4.2} l = 9 \times 10^{-16}$ $\Omega$ m$^2$, where $\rho_{4.2}$ is the resistivity at 4.2 K. The values of $\tau_E$ were estimated from the measured $T_c$ using $\tau_E = (12 \text{ nsec})(1.2/T_c)^3$ [see CC Eq. (1.1)]. The values of $\tau_S$ were estimated from the atomic concentration of Er, $n_{Er}$, using an exchange scattering rate inferred from the data of Craven *et al.*,[31] $\tau_S^{-1} = (1.9 \pm 0.4) \times 10^{13} n_{Er}$ sec$^{-1}$. We estimated $\Omega$ to within 5% from the measured area of the window in the SiO defining the injector junction and the measured film thickness, and used[32] $N(0) = 1.74 \times 10^{28}$ eV$^{-1}$ m$^{-3}$.

We estimated the order parameter in the AlEr film from a plot of $dV_i/dI_i$ vs $V_i$ using the voltages at which the minima corresponding to the sum and difference of the Al and AlEr order parameters occurred. We were able to measure the order parameter at temperatures up to a few mK of $T_c$ with an uncertainty of about 1 $\mu$V. The zero-voltage conductance of the detector junction, $g_{NS}$, was measured at voltages less than 10 nV from the $V_d$-$I_d$ characteristic obtained with the SQUID voltmeter.

## IV. EXPERIMENTAL RESULTS

The order parameter of the AlEr films followed the BCS temperature dependence to within a few mK of $T_c$. However, the magnitude was smaller than expected from the measured $T_c$, but never by more than 13%.

Typical measured values of $g_{NS}$ are shown in Fig. 2, along with the BCS curve.[33] The dip in the measured conductance as $\Delta/k_B T_c \to 0$ was also noted by Clarke and Paterson.[13] At lower temperatures, the values of $g_{NS}$ lie significantly above the BCS values, indicating that the quality of the very low resistance ($\sim$1 m$\Omega$) detector junctions was poor. However, previous work[13] indicates that the quality of the detector junction does not affect the measurement of $Q^*$ significantly, provided one uses the *measured* conductance normalized to its maximum value (at a temperature somewhat below $T_c$) in Eq. (2.8).

Figure 3 is a representative plot of $|V_d|$ vs $|I_i|$ for positive and negative injection currents. The structure below about 0.5 mA reflects the structure in the $I_i$-$V_i$ characteristic. At higher currents there is a slight asymmetry between the two curves, probably due to temperature gradients caused by heating in the injector junction, but the average value of $|V_d|$

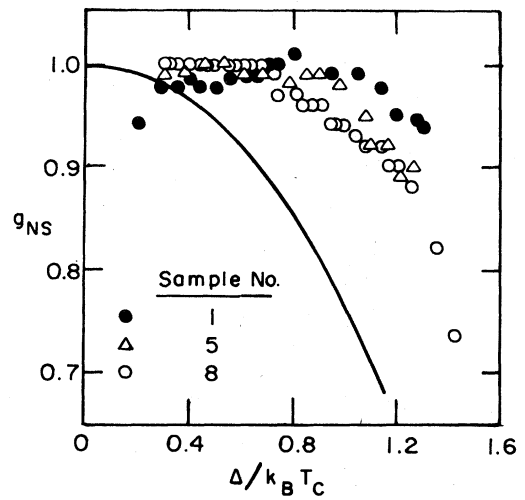


FIG. 2. Plot of typical experimental values of the detector junction conductance, $g_{NS}$, at low voltages. The solid line is the BCS value for a *N-I-S* tunnel junction.

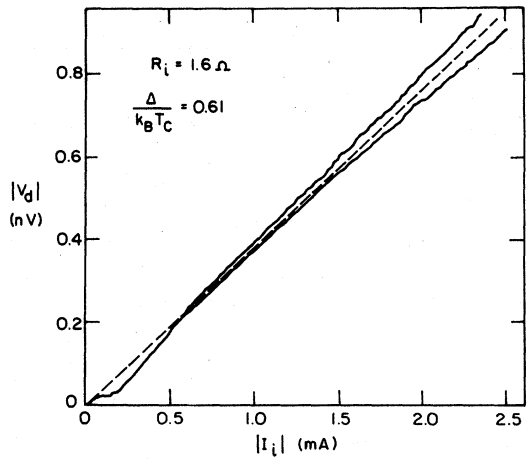


FIG. 3. Experimental plot of $|V_d|$ vs $|I_i|$. The two curves represent the two polarities of $I_i$ and $V_d$. The dashed line shows that, although there is some asymmetry between the two polarities, the average of $|V_d|$ is proportional to $|I_i|$ for sufficiently large injection voltage.

(dashed line) is proportional to $|I_i|$ for $|eV_i| \gg \Delta$. The value of $V_i/I_i$ in this high-voltage region is used with the measured values of $\Omega$ and $g_{NS}$ to obtain $1/F^*\tau_{Q^*}$ from Eq. (2.8).

Figures 4 and 5 show representative plots of $1/F^*\tau_{Q^*}$ vs $\Delta/k_BT_c$ for each impurity concentration.

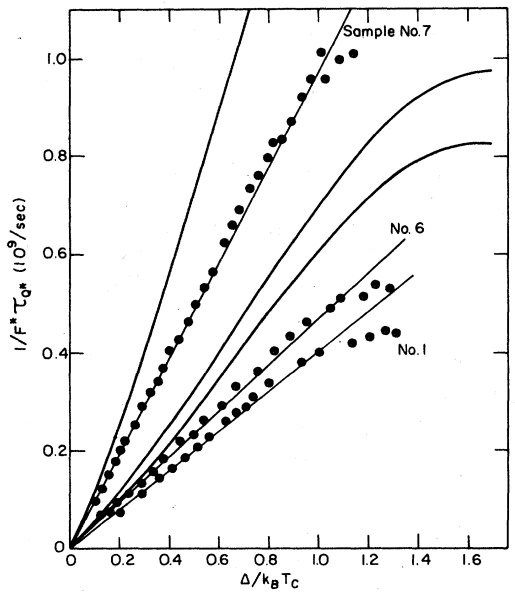


FIG. 4. Experimental values of $1/F^*\tau_{Q^*}$ vs $\Delta/k_BT_c$ for samples with Er concentrations of 21, 81, and 220 at. ppm, with straight lines drawn through the data by eye. The other curves, which represent computer solutions to the Boltzmann equation, have the same slope as the data in the limit $\Delta/k_BT_c \to 0$.

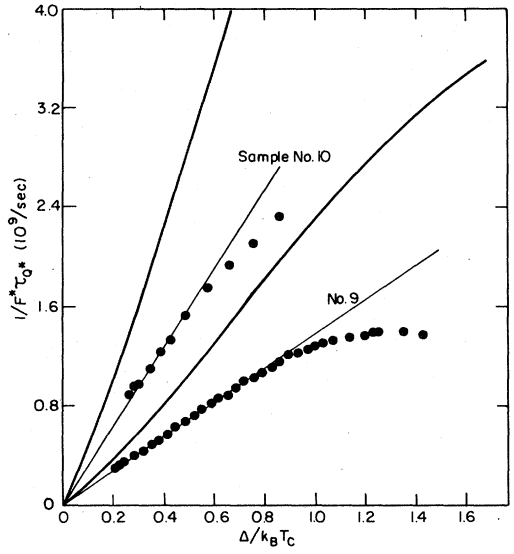


FIG. 5. Experimental values of $1/F^*\tau_{Q^*}$ vs $\Delta/k_BT_c$ for samples with Er concentrations of 520 and 1660 at. ppm with straight lines drawn through the data by eye. The other curves, which represent computer solutions to the Boltzmann equation, have the same slope as the data in the limit $\Delta/k_BT_c \to 0$.

In each case, $1/F^*\tau_{Q^*}$ is linear in $\Delta/k_BT_c$ up to a value of about 0.8 ($T \approx 0.92T_c$), tending to flatten off as $\Delta/k_BT_c$ increases further. The initial linear behavior is consistent with the SS result Eq. (2.10) provided one extrapolates the SS result to *substantially* higher values of $\Delta/k_BT_c$ than is justified *a priori*. This result is very surprising since the theory appears to fit the data when $\Delta \sim k_BT_c$, that is, when $\tau_{Q^*} \sim (\tau_E\tau_S)^{1/2}$, so that $(\tau_E/\tau_{Q^*}) \gg 1$. This limit is clearly outside the region in which the heuristic argument at the end of Sec. II can possibly be valid. As a further test of the applicability of the SS theory, in Fig. 6 we plot the measured values of the slope $S$ of the linear region for all samples versus the SS expression $(\pi/4\tau_E)(1+2\tau_E/\tau_S)^{1/2}$, using the value of $\tau_E$ listed in Table I, and the value of $\tau_S$ estimated from the impurity concentration, also listed in Table I. The general agreement is good, implying that the SS result [Eq. (2.10)] accurately describes the observed dependence of $1/F^*\tau_{Q^*}$ on $\Delta/k_BT_c$, $\tau_E$, and $\tau_E/\tau_S$ for $\Delta/k_BT_c \lesssim 0.8$, and confirming the exchange scattering rate per impurity inferred from Craven *et al.*[31]

The universal behavior of $1/F^*\tau_{Q^*}$ is clearly illustrated in Fig. 7, which shows $1/SF^*\tau_{Q^*}$ vs $\Delta/k_BT_c$ for one sample of each Er concentration. Although there is a spread in the results for the larger values of $\Delta/k_BT_c$, it is apparent that the data, normalized in this way, lie on a universal curve. We emphasize that this universal behavior holds true even for sam-

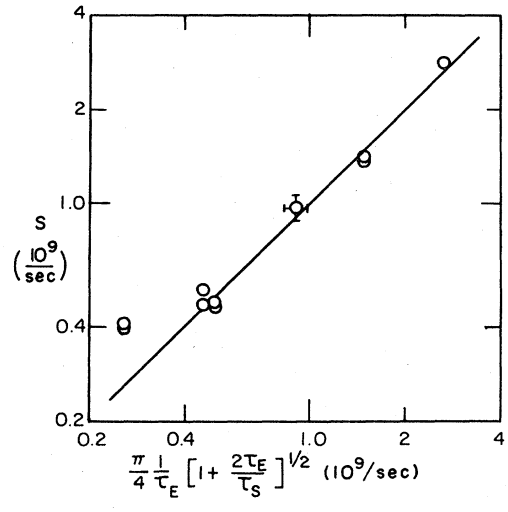


FIG. 6. Plot of $S$, the slope of $1/F^*\tau_{Q^*}$ vs $\Delta/k_BT_c$ for small $\Delta/k_BT_c$, for all samples. The quantity $(\pi/4\tau_E)(1+2\tau_E/\tau_S)^{1/2}$ is calculated for each sample by using the values of $\tau_E$ and $\tau_S$ (estimated) from Table I. The solid line has unity slope, and passes through the origin.

ple 10, for which gap smearing is quite large ($\hbar\tau_S^{-1} \gtrsim \frac{1}{2}\Delta$ for $\Delta/k_BT_c \lesssim 0.4$), thus lending experimental support to the SS criterion $\hbar^2\Gamma/\Delta^2\tau_E \gtrsim 1$ for gap smearing to affect $\tau_{Q^*}^{-1}$ appreciably.

We note in passing that this agreement between the SS theory and the data justifies the use of the SS result by CC in their hypothesis concerning the dependence of $\tau_E$ on $T_c$.

To compare rigorously the theory with the data for values of $\Delta/k_BT_c$ up to 1.4, and to check the range of validity of the SS result, we solved the Boltzmann equation numerically. The form of the equation and the results it provides are discussed in Sec. V.

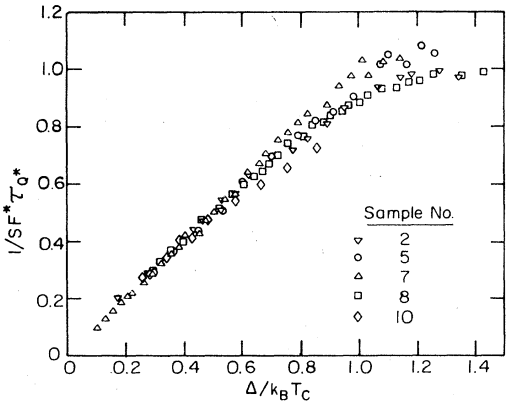


FIG. 7. Plot of $1/SF^*\tau_{Q^*}$ vs $\Delta/k_BT_c$ for one representative sample of each impurity concentration.

## V. CALCULATION OF THE CHARGE-IMBALANCE RELAXATION RATE IN THE PRESENCE OF MAGNETIC IMPURITIES

### A. Boltzmann equation

We seek a Boltzmann equation that describes a steady-state, spatially uniform charge imbalance generated by quasiparticle injection across a tunnel junction. We follow the general approach of CC, with the addition of a term to take into account exchange charge relaxation. We assume that the quasiparticle distribution function is independent of spin because the quasiparticle injection rate in independent of spin, and that it is independent of the direction of $\vec{k}$ because of the enormous elastic scattering rate. We can then label the distribution function for each state $\vec{k}$, $\vec{\sigma}$ by the appropriate value of $\epsilon = \pm(E^2-\Delta^2)^{1/2}$, where $\pm$ refer to states with $k \gtrless k_F$, and $E$ is the excitation energy referred to the chemical potential $\mu_s$. In the notation of CC, the Boltzmann equation is

$$\frac{\partial f_\epsilon}{\partial t} = G_\epsilon - G_{in\epsilon} - G_{s\epsilon} = 0 \ . \tag{5.1}$$

In Eq. (5.1), $G_\epsilon$ is the rate of quasiparticle injection into the state $\epsilon$. For simplicity, we assume that the injection is from a normal metal; the results are indistinguishable from those for a superconducting injection film at the high-injection voltages ($>>\Delta/|e|$) in which we are interested. The rate is

$$G_\epsilon = \tfrac{1}{2}R_0\{[f^0(E+eV_i)+f^0(E-eV_i)-2f^0(E)] + (\epsilon/E)[f^0(E-eV_i)-f^0(E+eV_i)]\} \ , \tag{5.2}$$

where $f^0$ is the Fermi function, $E=(\epsilon^2+\Delta^2)^{1/2}>0$, and $R_0 \equiv G_{NN}/2N(0)\Omega e^2$, with $G_{NN}$ the conductance of the injector junction when both films are normal.

In Eq. (5.1), $G_{in\epsilon}$ is the rate at which quasiparticles scatter out of the state $\epsilon$ due to inelastic scattering, and is given by CC in Eq. (2.16). This term is proportional to $\tau_E^{-1}$. The last term, $G_{s\epsilon}$, is the rate at which quasiparticles undergo elastic exchange scattering from state $\epsilon$ to all states $-\epsilon$. Since the elastic scattering rate due to gap anisotropy is very small compared with the exchange scattering rate in our samples, we shall neglect it. An expression for $G_{s\epsilon}$ can be obtained from Artemenko *et al.*,[34] but in the Appendix we give a more straightforward golden-rule derivation that does not involve Green's functions. The result is

$$G_{s\epsilon} = \frac{1}{\tau_S}\frac{\Delta^2}{E^2}\frac{E}{|\epsilon|}(f_\epsilon - f_{-\epsilon}) \ . \tag{5.3}$$

Note that the rate of exchange scattering that does not involve branch crossing is zero because the distribution function is independent of spin. In the rest of

this paper, references to exchange scattering refer to branch-crossing events.

The above collision integrals have been derived in the clean limit, where $\vec{k}$ is a good quantum number. Following Pethick and Smith,[9] we assume that the same expressions are valid in the dirty limit, provided that they are written in terms of $E$, which is still a good quantum number. These expressions are strictly applicable only for temperatures such that $\hbar\tau_S^{-1} \ll \Delta(T)$, because the smearing in the superconducting density of states has been neglected. However, if one accepts the SS criterion for the neglect of gap smearing on $\tau_{Q^*}$, $\hbar^2\Gamma/\Delta^2\tau_E \ll 1$, they may be applicable for temperatures much closer to $T_c$. We also emphasize that the full electron-phonon and exchange operators are used, rather than relaxation-time approximations; neither operator has been linearized in $\delta f_\epsilon$.

Finally, we note that for the small perturbations of interest in this paper, there is a temperature range $0.5 \lesssim T/T_c \leq 1$ in which one *can* linearize the Boltzmann equation in $\delta f_\epsilon$. It is easy to see by inspection of the generation and relaxation terms that in this case $\delta f_\epsilon$ is proportional to $R_0\tau_E$ for fixed $\tau_E/\tau_S$, $eV_i/k_BT_c$, and $\Delta/k_BT_c$. Consequently, $\tau_{Q^*}$ is independent of $R_0$, and its dependence on $\tau_E$ and $\tau_S$ is naturally characterized by the parameters $\tau_E$ and $\tau_E/\tau_S$.

### B. Computer solution of the Boltzmann equation

For convenience in the numerical solution of Eq. (5.1) we normalize $T$, $\epsilon$, $E$, $\Delta$, and $eV_i$ to $k_BT_c$. When the Boltzmann equation is written using these normalizations, it is clear that $f_\epsilon$ depends on $T/T_c$ but not $T_c$. We write the quasiparticle distribution function as $f_\epsilon = f^0 + \delta f_\epsilon$, where $f^0$ is the Fermi function at energy $+(\epsilon^2+\Delta^2)^{1/2}$. (In the notation of PS, $\delta f_\epsilon = \delta f_\epsilon^{\text{l.e.}}$, the deviation of $f_\epsilon$ from local equilibrium.) We rewrite the Boltzmann equation in terms of the longitudinal and transverse components of $\delta f_\epsilon$, $\delta f_\epsilon^L \equiv \frac{1}{2}(\delta f_\epsilon + \delta f_{-\epsilon})$ and $\delta f_\epsilon^T \equiv \frac{1}{2}(\delta f_\epsilon - \delta f_{-\epsilon})$. We make an initial guess at the values of $\delta f_\epsilon^L$ and $\delta f_\epsilon^T$ for values of $\epsilon$ from zero to some energy much larger than $\Delta$, $k_BT$, and $|eV_i|$, and use the Boltzmann equation to generate new values of $\delta f_\epsilon^L$ and $\delta f_\epsilon^T$. This procedure is iterated until a consistent solution is found. The value of the charge relaxation rate is then found from $\tau_{Q^*}^{-1} = \dot{Q}_i^*/Q^*$, where $\dot{Q}_i^*$ is calculated from Eq. (2.3) and $Q^* = 4N(0)\sum_{\epsilon>0} q_\epsilon \delta f_\epsilon^T$. The values of the various parameters used in the calculated results presented here are $\tau_E = 10$ nsec, 41 psec $\leq \tau_S \leq \infty$, $0.5 \leq T/T_c \leq 0.999\,999$, $V_i = 30\Delta(T)/e$, and $R_0 = 200$ sec$^{-1}$. [Typical experimental values are $\tau_E = 8$ nsec, 20 psec $\leq \tau_S \leq 3$ nsec, $0.75 \leq T/T_c \leq 0.999$, $V_i = 30\Delta(T)/e$, and $R_0 = 200$ sec$^{-1}$.]

We make several approximations in our computation: (i) The phonons are assumed to be in thermal equilibrium. Phonon trapping does not affect measurements of $\tau_{Q^*}$ because when a $2\Delta$ phonon breaks a pair the two quasiparticles generated on the average populate the two branches equally. (ii) The electron-phonon coupling parameter, $\alpha^2F(E)$, is taken to be quadratic in $E$. (iii) The nonequilibrium currents across the injector and detector junctions are small compared with $I_i$, and are neglected. (iv) The BCS value of $\Delta(T)$ is used. The magnetic impurities caused deviations from BCS behavior of at most a few percent. The change in $\Delta(T)$ caused by the nonequilibrium distribution of quasiparticles for all appropriate values of the parameters is also at most a few percent.

### C. Results of the computer calculation

Figure 8 shows calculated values of $1/F^*\tau_{Q^*}$, normalized to $(\pi/4\tau_E)(1+2\tau_E/\tau_S)^{1/2}$, vs $\Delta/k_BT_c$ for several values of $\tau_E/\tau_S$. The curves change by less than 1% when $R_0$ is increased by a factor of 10, confirming that the calculation is in the weak perturba-

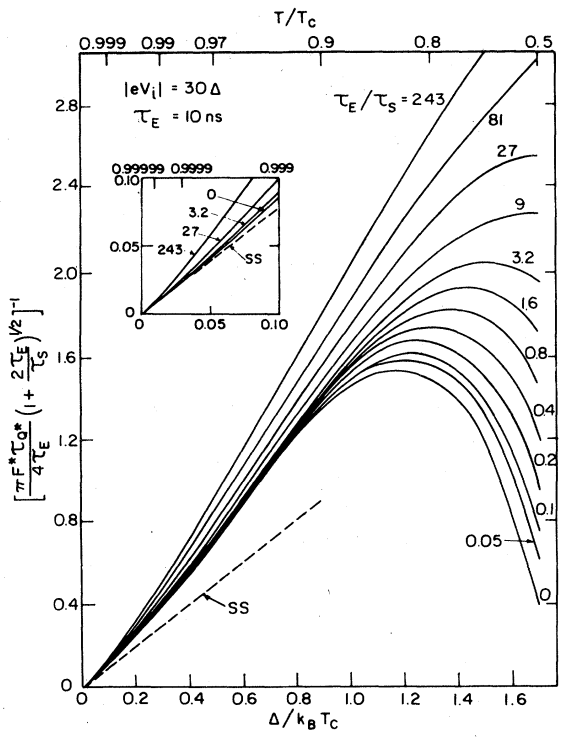


FIG. 8. Computer-generated values of $1/F^*\tau_{Q^*}$ normalized to $(\pi/4\tau_E)(1+2\tau_E/\tau_S)^{1/2}$ vs $\Delta/k_BT_c$. The curves approach the origin with unity slope. The dashed line is an extrapolation of the SS theory to low temperatures. The inset shows the region near the origin.

tion limit in this temperature range. The accuracy of these results has been checked in several ways. For $\tau_S^{-1}=0$, the results agree precisely with those of CC for all temperatures studied. For $\tau_E/\tau_S \leq 243$ and $\Delta/k_BT_c=0.003$ ($T/T_c=0.999\,999$), the results are within 3% of the SS result, Eq. (2.10). (See insert in Fig. 8.) In the experimentally inaccessible limit $\tau_E^{-1} \ll R_0 \ll \tau_S^{-1}$, $\Delta/k_BT_c \to 0$, and $|eV_i| \ll k_BT_c$, the results agree with the analytic result obtained by[35] PS from the Boltzmann equation:

$$\frac{1}{F^*\tau_{Q^*}}=\left(\frac{\Delta}{k_BT_c}\right)^2\frac{6}{\pi^2\tau_S} \qquad (5.4)$$

$$(\Delta/k_BT_c \to 0,\ \tau_E^{-1} \ll R_0 \ll \tau_S^{-1},\ |eV_i| \ll k_BT_c)\ .$$

We emphasize that, although some data were taken on sample 10 for $\hbar\tau_S^{-1} \lesssim \Delta$ where gap smearing should be large, there was no significant difference between values of $1/F^*\tau_{Q^*}$ vs $\Delta/k_BT_c$ for sample 10 and those for the other samples for which all of the data were taken where $\hbar\tau_S^{-1} \ll \Delta$. Therefore, the neglect of gap smearing in our calculation appears to be experimentally justified. Furthermore, if we assume that the SS requirement for gap smearing to have no effect on $\tau_{Q^*}^{-1}$ is correct, namely, $\hbar\tau_S^{-1} < \Delta(T)(\tau_E/2\tau_S)^{1/2}$, we would expect our calculations to be applicable in this range also.

Note that, for $\Delta/k_BT_c < 1$, the calculated values of $1/F^*\tau_{Q^*}$ lie above the SS result (except at $\Delta/k_BT_c=0$), by an amount that increases with $\tau_E/\tau_S$. This discrepancy persists to $\tau_E/\tau_S=0$, as was found earlier by CC. Furthermore, for all values of $\Delta/k_BT_c$, the calculated values of $[(\pi F^*\tau_{Q^*}/4\tau_E)(1+2\tau_E/\tau_S)^{1/2}]^{-1}$ increase monotonically with $\tau_E/\tau_S$. Because these normalized values of $1/F^*\tau_{Q^*}$ depend so markedly on $\tau_E/\tau_S$, they do not show the universal behavior exhibited by the data. This can be seen readily by comparing the calculated quantity in Fig. 8 with the equivalent experimental quantity in Fig. 7.

It is interesting to examine the effects of exchange scattering on the distribution function. Figure 9 shows $\delta f_\epsilon^T$ vs $\epsilon/k_BT_c$ for $R_0=200$ sec$^{-1}$, $\tau_E^{-1}=10^8$ sec$^{-1}$, and, for comparison, $f^0$ vs $\epsilon/k_BT_c$. The perturbation is again everywhere much smaller than $f^0$, so that $\delta f_\epsilon^T$ is proportional to $R_0\tau_E$ for fixed $\tau_E/\tau_S$, $\Delta/k_BT_c$, and $eV_i/k_BT_c$. As expected, $\delta f_\epsilon^T$ decreases at all energies as $\tau_E/\tau_S$ increases. Furthermore $\delta f_\epsilon^T$ decreases more at low energies than at high energies, and the peak therefore moves to higher energies, because the exchange collision operator [Eq. (5.3)] is proportional to $\Delta^2/E|\epsilon|$. This is a graphic demonstration of the picture in which the low-lying excitations are rapidly relaxed by exchange scattering, thus depleting the charge imbalance at low energies because of the relatively slow rate at which high-energy-injected quasiparticles can be cooled into this energy range by phonon scattering. For energies greater

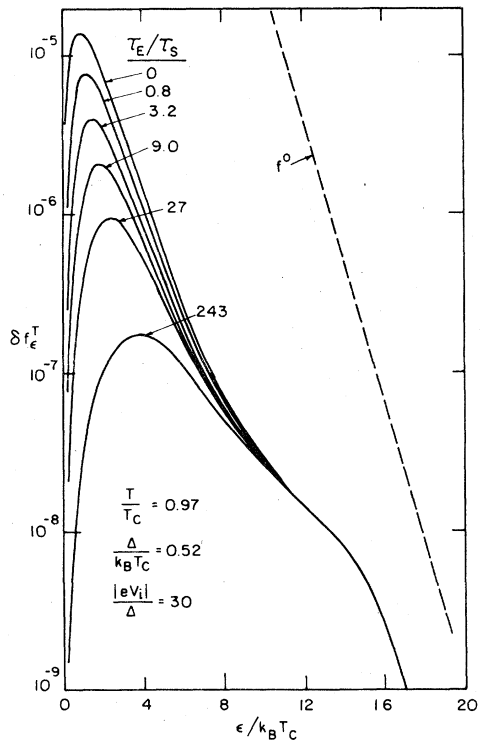


FIG. 9. Numerical results for $\delta f_\epsilon^T$ for several values of $\tau_E/\tau_S$ with $R_0=200$ sec$^{-1}$, and $\tau_E^{-1}=10^8$ sec$^{-1}$.

than $|eV_i|$, $\delta f_\epsilon^T$ decreases as $\exp(-\epsilon/k_BT)$ because the number of phonons which can scatter a quasiparticle from $E \approx k_BT$ to $E' \gtrsim |eV_i|$ is proportional to $\exp[-(E'-E)/k_BT]$. For the injection voltage used in Figs. 8 and 9, $|eV_i|/\Delta(T)=30$, which lies near the middle of the range used in the measurement of $\tau_{Q^*}$, $25\Delta \lesssim |eV_i| \lesssim 40\Delta$, the shape of both the $\delta f_\epsilon^T$ and $1/F^*\tau_{Q^*}$ curves is essentially independent of $|eV_i|/k_BT_c$. This is because the excess quasiparticles are injected at such large energies ($\gg k_BT$) that they must cool somewhat before they can undergo scattering events that relax $Q^*$. This cooling erases the memory of the energy at which each quasiparticle was injected. The dependence of $\delta f_\epsilon^T$ on $\epsilon$ would be affected by $|eV_i|$ if $|eV_i|+k_BT$ were less than or comparable with the energy at the peak of $\delta f_\epsilon^T$.

The longitudinal distribution, $\delta f_\epsilon^L$, is independent of $\tau_E/\tau_S$ in the temperature range where nonlinear effects are negligible.

### D. Comparison of computer results with experimental data

In Figs. 4 and 5 we plot curves computed using the values of $\tau_E$ and $\tau_S$ (fitted) from Table I along with the experimental data. The values of $\tau_S$ are chosen to give the computed curves the same slope as the data for small $\Delta/k_BT_c$, that is, by fitting the SS result,

Eq. (2.10) to the data. It is immediately clear that, rather than providing a better fit to the data than the extrapolated SS result, the computed curves give a much worse fit. We have tried various other fitting procedures, for example, choosing $\tau_S$ to force the computed curves to intersect the data at $\Delta/k_BT_c=0.5$, but have not been able to produce an acceptable fit. We note that the values of $\tau_S$ used in the computed curves (last column of Table I) are all within a factor of about 2 of the values estimated (second to last column) from the measured Er concentration; most of them are actually in even better agreement. Thus, the values of $\tau_S$ obtained from our fitting procedure appear to be very reasonable, and their overall consistency is confirmed by the straight-line fit in Fig. 6.

This marked discrepancy between the data and the computed curves is extremely puzzling. It should be pointed out that the discrepancy cannot be explained by invoking an additional charge-relaxation mechanism in the experiments, for example, Andreev reflection[36] at a nonuniform gap or at the surface of the film, because the experimental rate $1/F^*\tau_{Q^*}$ lies substantially below, rather than above the computed rate. Another possible difficulty in the theory concerns the assumption that the Er atoms do not interact with each other. However, if such interactions were important we would expect to see some saturation of the increase of $1/F^*\tau_{Q^*}$ with $n_{\rm Er}$ at the highest Er concentration, but no such saturation is evident from the data (see Fig. 6). Furthermore, it is known that in superconductors containing magnetic impurities, impurity-impurity interactions are small until the impurity concentration is large enough to reduce the transition temperature to typically one-half that of the pure superconductor.[37] We estimate that $T_c$ was reduced by only 6% for the sample with the highest Er concentration, again implying that these interactions are negligible. Further, we expect no Kondo anomalies because $g$-shift measurements[38] have shown that the exchange constant is positive for Er impurities in Al. Thus, we expect that the exchange scattering rate $\tau_S^{-1}$ should not be a strong function of energy or temperature. We conclude that either the collision operator for exchange scattering, Eq. (5.3), is inappropriate for charge relaxation or that the Boltzmann equation is not an adequate description of charge relaxation in the presence of magnetic impurities. We are left with the undisputable fact that the Schmid-Schön result, Eq. (2.10), provides a very satisfactory fit to the data over a much wider temperature range than can reasonably be expected.

## VI. CONCLUDING SUMMARY

We have measured $1/F^*\tau_{Q^*}$ as a function of $\Delta/k_BT_c$ in AlEr alloys in which the Er is a magnetic impurity that induces elastic exchange charge relaxation. Values of the exchange scattering rate ranged from about $10^9$ to $5\times10^{10}$ sec$^{-1}$. For all concentrations of Er, $1/F^*\tau_{Q^*}$ increased linearly with $\Delta/k_BT_c$ for $\Delta/k_BT_c\lesssim0.8$, and less rapidly for higher values of $\Delta/k_BT_c$. The slope of the linear region was $(\pi/4\tau_E)(1+2\tau_E/\tau_S)^{1/2}$, in agreement with the SS result. The Boltzmann equation, with an appropriate term for exchange charge relaxation, was solved numerically, and the values of $1/F^*\tau_{Q^*}$ were compared with the experimental data. The computed curves did not have the same temperature dependence as the data for any concentration of Er. Furthermore, they did not show the universal behavior evident in the data. This disagreement implies that either the usually accepted expression for exchange charge relaxation is incorrect or that the Boltzmann equation cannot be used in this type of calculation. It would be of considerable interest to make accurate measurements of $1/F^*\tau_{Q^*}$ in the presence of other pair-breaking mechanisms, for example, an applied magnetic field or supercurrent, to investigate whether the discrepancy concerns pair-breaking effects in general or magnetic impurities in particular.

## ACKNOWLEDGMENTS

We are grateful to C. C. Chi, O. Entin-Wohlman, R. Orbach, A. Schmid, G. Schön, and H. Smith for helpful conversations. One of the authors (T.R.L.) gratefully acknowledges a fellowship from IBM. This work was supported by the Division of Materials Sciences, Office of Basic Energy Sciences, U.S. DOE under Contract No. W-7405-Eng-48.

## APPENDIX

We derive an expression for $G_{s\epsilon}$ the net exchange branch-crossing scattering rate, which appears in Eq. (5.1). Following Abrikosov and Gor'kov [25] (AG), we assume that the magnetic impurities interact with each conduction electron according to

$$H_{\rm int}=\sum_j U(\vec{r}-\vec{r}_j)+J(\vec{r}-\vec{r}_j)\,\vec{S}_j\cdot\vec{\sigma}\quad . \tag{A1}$$

In this expression, $U$ is the usual elastic scattering potential, $J$ is the exchange potential, $\vec{S}_j$ is the impurity spin at $\vec{r}_j$, and $\vec{\sigma}$ is the Pauli vector matrix. The impurity spins are assumed to have equal magnitudes and to be randomly oriented and distributed. Writing this perturbation in second-quantized form, we obtain

$$\begin{aligned}H_{\rm int}=\sum_{\vec{p},\vec{p}'}\,[&I_{\vec{p}-\vec{p}'}\tilde{U}_{\vec{p}-\vec{p}'}(a^\dagger_{\vec{p}\uparrow}a_{\vec{p}'\uparrow}+a^\dagger_{\vec{p}\downarrow}a_{\vec{p}'\downarrow})\\&+\tilde{J}_{\vec{p}-\vec{p}'}\tilde{S}^z_{\vec{p}-\vec{p}'}(a^\dagger_{\vec{p}\uparrow}a_{\vec{p}'\uparrow}-a^\dagger_{\vec{p}\downarrow}a_{\vec{p}'\downarrow})\\&+\tilde{J}_{\vec{p}-\vec{p}'}(\tilde{S}^+_{\vec{p}-\vec{p}'}a^\dagger_{\vec{p}\downarrow}a_{\vec{p}'\uparrow}+\tilde{S}^-_{\vec{p}-\vec{p}'}a^\dagger_{\vec{p}\uparrow}a_{\vec{p}'\downarrow})\,]\end{aligned} \tag{A2}$$

In this equation,

$$\tilde{U}_{\vec{p}-\vec{p}'}=\frac{1}{\Omega}\int e^{i(\vec{p}-\vec{p}')\cdot\vec{r}}U(\vec{r})\,d\vec{r}\ , \tag{A3}$$

$$\tilde{J}_{\vec{p}-\vec{p}'}=\frac{1}{\Omega}\int e^{i(\vec{p}-\vec{p}')\cdot\vec{r}}J(\vec{r})\,d\vec{r}\ , \tag{A4}$$

$$\tilde{S}^{z,\pm}_{\vec{p}-\vec{p}'}=\sum_j e^{i(\vec{p}-\vec{p}')\cdot\vec{r}_j}S^{z,\pm}_j\ , \tag{A5}$$

$$I_{\vec{p}-\vec{p}'}=\sum_j e^{-i(\vec{p}-\vec{p}')\cdot\vec{r}_j}\ , \tag{A6}$$

$a^\dagger$ and $a$ are the creation and annihilation operators for electrons, and $\Omega$ is the volume. The first term of Eq. (A2) is absorbed into the part of the Hamiltonian which includes ordinary potential scattering from nonmagnetic impurities. The diagonal part of the second term shows explicitly that the electron states $\vec{p}\uparrow$ and $-\vec{p}\downarrow$ have different energies. This breaks the degeneracy between the two members of a Cooper pair, giving the pairs a finite lifetime, and resulting in a smeared density of states, an altered dependence of $\Delta$ on $T$, and a reduced $T_c$. Since we are treating the interaction as a perturbation on the BCS state, we neglect these effects: This approximation is justified for a sufficiently low impurity concentration. In our view, charge relaxation is due to both elastic non-spin-flip branch-crossing scattering events arising from the off-diagonal part of the second term[39] in Eq. (A2), and to elastic spin-flip branch-crossing scattering events arising from the third term in Eq. (A2). In this paper, we use the term "exchange scattering" to refer to such scattering events. (Another common convention in the literature is to refer to such events as "spin-flip scattering.") Note that, here, energy conservation forbids pair breaking and recombination events such as are caused by inelastic quasiparticle scattering from phonons. When we replace the one-electron operators in this term with the appropriate Bogoliubov operators and use the golden rule to calculate the transition from a state $\vec{k}>\vec{k}_F$, spin $\downarrow$ to all other states $\vec{l}<\vec{k}_F$, spin $\uparrow$ and $\downarrow$, we obtain

$$\dot{f}^{>}_{\vec{k}\downarrow}\big|_s=\frac{2\pi}{\hbar}n_i\Omega S(S+1)\sum_{\vec{l}<\vec{k}_F}|\tilde{J}_{\vec{l}+\vec{k}}|^2\delta(E_{\vec{l}}-E_{\vec{k}})\frac{\Delta^2}{E^2_{\vec{k}}}\left[\tfrac{1}{3}(f^{<}_{\vec{l}\downarrow}-f^{>}_{\vec{k}\downarrow})+\tfrac{2}{3}(f^{<}_{\vec{l}\uparrow}-f^{>}_{\vec{k}\downarrow})\right]\ . \tag{A7}$$

The factor $\frac{1}{3}n_i\Omega S(S+1)$, where $n_i$ is the number of magnetic impurities per unit volume and $S$ is the magnitude of the impurity spin, is the ensemble average of $|\tilde{S}^z_{\vec{p}+\vec{p}'}|^2$; $\frac{2}{3}n_i\Omega S(S+1)$ is the average of $|\tilde{S}^-_{\vec{p}+\vec{p}'}|^2$. The factor $\Delta^2/E^2_{\vec{k}}$ is the coherence factor for exchange scattering from one branch to the other (see Sec. II). The Fourier transform of the exchange potential, $\tilde{J}_{\vec{q}}$, is expected to be nearly constant for the range of momentum transfers of interest here, $0\leq|\vec{q}|\lesssim 2k_F$. Remembering that $f_{\vec{k}\uparrow}$ is in fact independent of spin and of the direction of $\vec{k}$, we can write Eq. (A7) in the form

$$\dot{f}_\epsilon\big|_s=\frac{2\pi}{\hbar}n_iS(S+1)(\Omega J)^2N(0)\times\frac{E}{|\epsilon|}\frac{\Delta^2}{E^2}(f_{-\epsilon}-f_\epsilon)\ , \tag{A8}$$

where $J^2$ is the angular average of $|\tilde{J}_{\vec{l}+\vec{k}}|^2$, $E/|\epsilon|$ is the normalized density of states in the superconductor, and $N(0)$ is the normal-state density of states per unit volume for a single spin. Since the exchange potential $J(\vec{r})$ is localized to roughly an atomic volume, it is clear from Eq. (A4) that $\Omega J$ is independent of $\Omega$.

The exchange scattering rate, $\tau_S^{-1}$, is defined as the temperature- and energy-independent coefficient of $(f_{-\epsilon}-f_\epsilon)$, so that we obtain finally

$$G_{s\epsilon}\equiv-\dot{f}_\epsilon\big|_s=\frac{1}{\tau_S}\frac{\Delta^2}{E|\epsilon|}(f_\epsilon-f_{-\epsilon})\ , \tag{A9}$$

where

$$\frac{1}{\tau_S}=\frac{2\pi}{\hbar}n_iS(S+1)(\Omega J)^2N(0)\ . \tag{A10}$$

Equation (A9) agrees with Artemenko *et al.*[34] The result, Eq. (A10), disagrees with the AG expression for $\tau_S^{-1}$ by a numerical factor. At first glance, this is not surprising because AG calculated equilibrium properties such as the depression of the transition temperature, $\delta T_c$, and not quasiparticle collision rates. However, it is known[8,40] that, in fact, the same rate, $\tau_S^{-1}$, should appear in Eq. (A9) as appears in AG Eq. (22) for $\delta T_c$. Therefore, values of $\tau_S^{-1}$ inferred from measurements of $\delta T_c$ by Craven *et al.*[31] are the appropriate values to use in Eq. (A9). We do not know why our result differs from that of AG, but we note that at least two other expressions[41,42] for $\tau_S^{-1}$ are available in the literature that differ from the AG result, from each other, and from Eq. (A10).

Entin-Wohlman and Orbach[43] also derived an expression for $G_{s\epsilon}$ using the golden rule to calculate scattering rates. However, they worked in the particle representation in which the behavior of the superconducting excitations is not clear. Their result would agree with ours if they had not omitted the factor $E/|\epsilon|$ in their Eq. (12).

[1]J. Clarke, Phys. Rev. Lett. 28, 1363 (1972).
[2]A. B. Pippard, J. G. Shepherd, and D. A. Tindall, Proc. R. Soc. London Ser. A 324, 17 (1971).
[3]T. Y. Hsiang and J. Clarke, Phys. Rev. B 21, 945 (1980).
[4]D. J. Van Harlingen, Bull. Am. Phys. Soc. 25, 411 (1980).
[5]J. Clarke, B. R. Fjordbøge, and P. E. Lindelof, Phys. Rev. Lett. 43, 642 (1979).
[6]W. J. Skocpol, M. R. Beasley, and M. Tinkham, J. Low Temp. Phys. 16, 145 (1974).
[7]M. Tinkham, Phys. Rev. B 6, 1747 (1972).
[8]A. Schmid and G. Schön, J. Low Temp. Phys. 20, 207 (1975).
[9]C. J. Pethick and H. Smith, Ann. Phys. 119, 133 (1979).
[10]J. R. Waldram, Proc. R. Soc. London Ser. A 345, 231 (1975).
[11]A. M. Kadin, L. N. Smith, and W. J. Skocpol, J. Low Temp. Phys. 38, 497 (1980).
[12]Strictly speaking, $\tau_E$ is an energy-dependent scattering time, defined in Ref. 8, Eq. (43). Since it is nearly constant for energies less than $\sim k_B T_c$, we use the symbol, $\tau_E$, to represent this constant value.
[13]J. Clarke and J. L. Paterson, J. Low Temp. Phys. 15, 491 (1974).
[14]M. V. Moody and J. L. Paterson, J. Low Temp. Phys. 34, 83 (1979).
[15]C. C. Chi and J. Clarke, Phys. Rev. B 19, 4495 (1979); 21, 333 (1980).
[16]A. R. Long, J. Phys. F 3, 2023 (1973).
[17]I. Schuller and K. E. Gray, Solid State Commun. 23, 337 (1977).
[18]K. E. Gray, A. R. Long, and C. J. Adkins, Philos. Mag. 20, 273 (1969).
[19]L. N. Smith and J. M. Mochel, Phys. Rev. Lett. 35, 1597 (1976).
[20]C. C. Chi and D. N. Langenberg, Bull. Am. Phys. Soc. 21, 403 (1976); (unpublished).
[21]S. B. Kaplan, C. C. Chi, D. N. Langenberg, J-J. Chang, S. Jafarey, and D. J. Scalapino, Phys. Rev. B 14, 4854 (1976).
[22]W. E. Lawrence and A. B. Meador, Phys. Rev. B 18, 1154 (1978).
[23]A. M. Kadin, W. J. Skocpol, and M. Tinkham, J. Low Temp. Phys. 33, 481 (1978).
[24]T. Y. Hsiang, Phys. Rev. B 21, 956 (1980).
[25]A. A. Abrikosov and L. P. Gor'kov, Zh. Eksp. Teor. Fiz. 39, 1781 (1960) [Sov. Phys. JETP 12, 1243 (1961)].
[26]J. Bardeen, L. N. Cooper, and J. R. Schrieffer, Phys. Rev. 108, 1175 (1957).
[27]C. J. Pethick and H. Smith, J. Phys. C (in press).
[28]In the Appendix, we present a golden-rule calculation of the net rate $G_{s\epsilon}$ at which quasiparticles undergo exchange scattering from state $\epsilon$ to all states $-\epsilon$, which yields:

$$G_{s\epsilon} = \frac{1}{\tau_S}\frac{\Delta^2}{E^2}\frac{E}{|\epsilon|}(f_\epsilon - f_{-\epsilon}) \ .$$

This result agrees with the Green's-function calculation of Artemenko *et al.* (Ref. 34). Pethick and Smith (Ref. 27) used this expression to obtain Eq. (2.12). The Schmid and Schön (Ref. 8) result, Eq. (2.10), differs from the PS result because SS made the simplifying assumption that the density-of-states factor, $E/|\epsilon|$, could be set equal to 1. Schön (private communication) later showed that when this assumption is not made, the SS result for $1/F^*\tau_{Q^*}$ is affected by less than 3%.
[29]G. I. Rochlin, Rev. Sci. Instrum. 41, 73 (1970).
[30]F. R. Fickett, Cryogenics 11, 349 (1971).
[31]R. A. Craven, G. A. Thomas, and R. D. Parks, Phys. Rev. B 4, 2185 (1971).
[32]K. A. Gschneidner, Solid State Phys. 16, 275 (1964).
[33]S. Bermon (unpublished).
[34]S. N. Artemenko, A. F. Volkov, and A. V. Zaitsev, J. Low Temp. Phys. 30, 487 (1978).
[35]C. J. Pethick and H. Smith (private communication).
[36]A. F. Andreev, Zh. Eksp. Teor. Fiz. 46, 182 (1964) [Sov. Phys. JETP 19, 1228 (1964)].
[37]D. M. Ginsberg, Phys. Rev. B 15, 1315 (1977).
[38]C. Rettori, D. Davidov, R. Orbach, E. P. Chock, and B. Ricks, Phys. Rev. B 7, 1 (1973).
[39]We thank O. Entin-Wohlman for pointing this out.
[40]O. Entin-Wohlman and R. Orbach, Ann. Phys. 116, 35 (1978).
[41]P. G. DeGennes, *Superconductivity of Metals and Alloys* (Benjamin, New York, 1966), p. 264.
[42]K. Maki, in *Superconductivity*, edited by R. D. Parks (Marcel Dekker, New York, 1969), p. 1037.
[43]O. Entin-Wohlman and R. Orbach, Phys. Rev. B 19, 4510 (1979).